Transactions on Engineering Sciences vol 25, © 1999 WIT Press, www.witpress.com, ISSN 1743-3533

A critical evaluation of residual stresses in spheroidal graphite cast iron due to mechanical testing

H.W. Theunissen, D.G. Hattingh, J Maczek, A. Els-Botes
Department of Mechanical Engineering, Port Elizabeth Technikon, Private Bag X6011, Port Elizabeth, South Africa
EMail: danieh@ml.petech.ac.za

Abstract

The understanding of the relationship between residual stresses and the effects of mechanical testing on these stresses needs to be evaluated to develop a testing method to ensure the separation of Grey Cast Iron and Spheroidal Graphite (SG) Cast Iron for Automotive Safety Critical Components. Residual Stresses in manufactured components are those stresses that exist without prior application of service or external loads[i]. Virtually all manufacturing and surface treatments induce residual stresses into a component which may either be beneficial or detrimental to the mechanical properties. This paper investigates the effect of an applied load on the residual stresses within spheroidal graphite castings. In order to measure the residual stresses present by means of the Centre Hole Drilling Method, the locked-in stresses must be relieved by removing material to enable a sensor to register the change in strain. In the final analysis the data will assist with the development of a test specification whereby Safety Critical Cast Components can be load tested without inducing detrimental stresses into a spheroidal Graphite Casting, but would cause failure of a Grey Casting.

1 Introduction

Residual Stresses are internal stresses that are present in almost all components that are manufactured, heat-treated or assembled. However, their effects are often not evident until the component is subjected to an external load or exposed to an adverse environment. Residual Stresses are a phenomenon that have been given many names and are receiving increased attention from the engineering research and design community. Many opportunities for the optimisation of design and manufacturing parameters are directly dependent on the better understanding of residual stresses[ii].

This study of residual stresses in spheroidal graphite cast iron arose from a local foundry that established a need to develop a more reliable test procedure for its Cast Safety Critical Automotive Components to compliment its current ultra-sonic testing.

2 Test Method

The test requires the destruction of grey cast iron specimens, which result from inadequate inoculation, but induce no detrimental stresses into a spheroidal graphite cast iron specimen. This test would then eliminate the grey cast iron components from the system and only allow SG specimens to proceed to the next phase of manufacture. The test to which the components were subjected, was simply the application of a predetermined load at a specific location, as illustrated in figure 1, resulting in the destruction of the grey cast iron specimens.

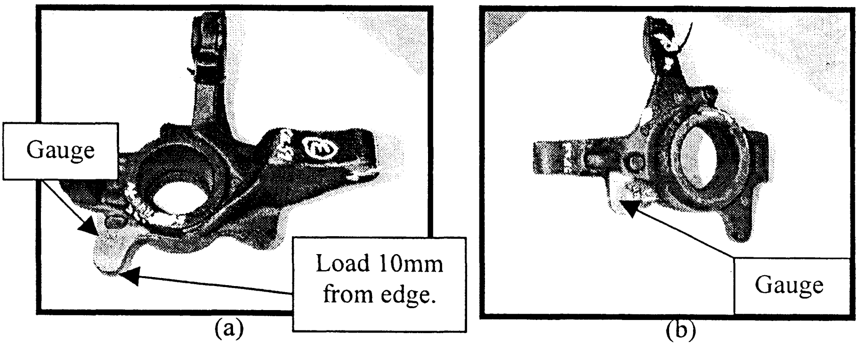

Figure 1: Arrows indicates the point of application of the strain gauges.
(a) Shows the strain gauge and where the test load was applied
(b) Shows the reference gauge for components CCC58/59

This investigation considered four components, each consisting of ten individual specimens, five being right hand side and the other five being left hand side automotive components. The test load for each of the components was determined by performing destructive load tests on grey cast iron components with the same geometry as that of the SG cast iron components.

A 'before and after' residual stress measurement was taken at the area of the load application assessing any variation in the residual stress magnitude due to the applied test load, see figure 1. However, due to the semi-destructive nature of the drilling method and the relaxing of the stresses around the hole due to the drilling, the same specimen could not be used. To overcome this, a number of specimens that were not subjected to the test load were used to establish the residual stresses present. The components tested in this investigation are listed in table 1.

Component	Description	Test Load
MA 69	Right Hand Side	0
MA 70	Left Hand Side	46 kN
CCC 58	Right Hand Side	0
CCC 59	Left Hand Side	38 kN

Table 1: Test Components.

3 Residual Stress Measurement

The Automatic Centre Hole High Speed Drilling method of residual stress measurement was chosen over other methods because of its ability to determine the residual stress distribution with depth, ease of operation and cost effectiveness. The evaluation software enables on-line measurement, while the change-of-strain measurements, the principal stresses of the plane residual stress state and their orientation can be viewed on the monitor in relation to the drilled depth. The equipment also allows for a quick and accurate alignment of the end mill to the drilling location as well as easy measurement of the hole diameter after drilling.

3.1 Description of Equipment and Drilling Procedure

The measurement of residual stresses require the internal stresses to be relieved by means of the destructive removal of successive layers of material. The equipment used was an Automatic Centre Hole Drilling device using a high-speed end mill is illustrated in figure2.

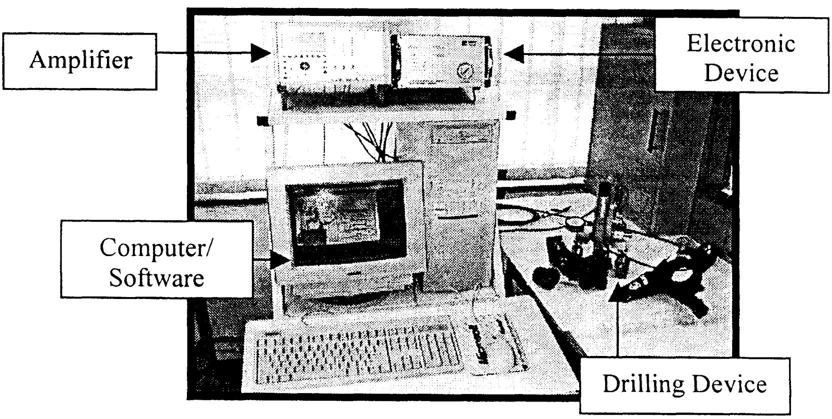

Figure 2: RESTAN Drilling Equipment.

Transactions on Engineering Sciences vol 25, © 1999 WIT Press, www.witpress.com, ISSN 1743-3533

The Residual Stress Equipment (RESTAN) consists of four major components:

3.1.1. Drilling Device

This drilling device houses an air turbine motor into which an inverted end mill is taper locked. The turbine rotates at about 300 000rpm at a pressure of 4.5 bar. To enable accurate alignment, the device consists of an optical aligning device to align the end mill to the centre of strain gauge's drilling location. The head is attached to the main frame via a V-slide and rack and pinion which allows for the quick setting of the end mill to the strain gauge drilling location. The frame is controlled by a stepper motor, which allows for computer controlled feed of the end mill through the centre of the strain gauge into the specimen.

3.1.2. Amplifier

The amplifier that was used for the measurements was a MGC amplifier, manufactured by HBM, which is computer controlled during the drilling operation. The three gauge rosette was wired to the amplifier using a four-lead quarter bridge circuit and in conjunction with the amplifier, recorded the strain magnitudes after each incremental step (cut).

3.1.3. Electronic Device

The function of the Electronic Device is to interface the computer signals, the solenoid valve controlling the air supply to the turbine motor and the stepper motor.

3.1.4. Computer/Software

SINT Technology of Italy developed the software in collaboration with HBM of Germany. This software controls the electronic unit and the MGC amplifier, as well as the processing of the strain data according to the number of incremental steps when the drilling operation is completed.

3.1.5. Strain Gauges

The measurements were taken using a Micro-Measurements EA-06-062RE-120 3-grid Rosette strain gauge as illustrated in figure 3.

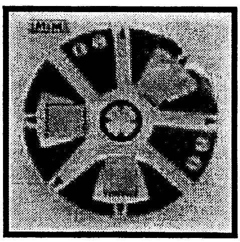

Figure 3: Micro Measurement's EA-06-062RE-120
3 grid Rosette Strain Gauge.

3.2 Measurement Procedure

The strain gauge was applied at the predetermined load point on each sample. The three grids were connected to the MGC amplifier after which, the Drilling Device was positioned over the specimen and drilling head aligned and levelled to the drilling location on the strain rosette. The feet of the Drilling Device were secured to the worktable and the end mill was brought as close as possible to the strain rosette and locked in this position as illustrated in figure 4.

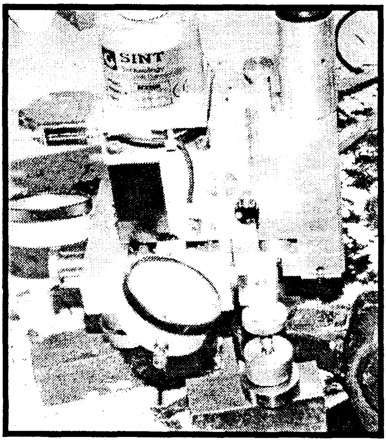

Figure 4: Positioning of the Drilling Head
on Strain Gauge Surface

The drilling parameters such as, number of incremental steps, depth as well as the delay time (interval between cuts) were predetermined and entered into the software. After the gauges were zeroed, drilling commenced. The holes were drilled to a depth of 2mm in 30 steps with the depths increasing incrementally from 0.01mm to 0.13mm. When the drilling was completed, the eccentricity of the hole was measured using the optical device in accordance with the requirements set out in ASTM E837.94 (a). These measurements were entered into the software for the final data processing of the strain results corresponding to their incremental depths.

3.3 Nomenclature

D_o = hole diameter
D = gauge circle diameter
Z = depth of hole
E = Young's modulus
$\overline{A}$; $\overline{B}$ = geometric constants as determined by ASTM 837.94(a)
$\overline{a}$; $\overline{b}$ = data reduction coefficients
α = angle from the first principal strain from first strain gauge

$\varepsilon_a; \varepsilon_b; \varepsilon_c$ = relieved strains values, where a, b & c correspond with the grids 1,2 &3.

$\sigma_{max}\ \sigma_{min}$ = maximum and minimum principal stresses

3.4 Calculation of Results

The principal stresses were determined according to the ASTM 837.94(a)[vi] method of calculation.

Principal Stresses:

$$\sigma_1 \,\&\, \sigma_2 = \frac{\varepsilon_c + \varepsilon_a}{4\overline{A}} \pm \frac{\sqrt{(\varepsilon_c - \varepsilon_a)^2 + (\varepsilon_c + \varepsilon_a - 2\varepsilon_b)^2}}{4\overline{B}} \tag{1}$$

Principal Angle:

$$\tan 2\alpha = \frac{(\varepsilon_c + \varepsilon_a - 2\varepsilon_b)}{\varepsilon_c - \varepsilon_a} \tag{2}$$

$$\text{where: } \overline{a} = \frac{2E\overline{A}}{1+\nu} \quad \text{and: } \overline{b} = 2E\overline{B} \tag{3}$$

4 Results

Figure 5 illustrates the typical residual stresses present at full depth in loaded and unloaded specimens. This allowed for the establishment of a residual stress range for any specific set of components. The results for the unloaded and loaded specimens all fell within this range.

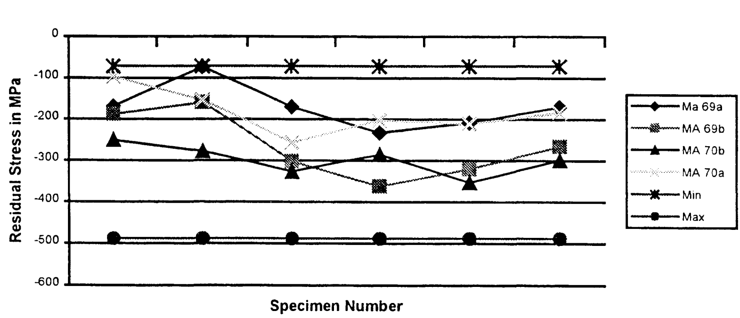

Figure 5: Range for Residual Stresses, Max –487MPa Min –72MPa

The hardness and residual stress results for two of the specimens tested are shown in figure 6. The graph illustrating the extreme (greatest maximum and least maximum) residual stress results of these two specimens tested, while the mean of the two is also plotted. It should be noted that specimen MA 70_2a, loaded to 46kN, produced the lowest residual stresses and specimen CCC 58_2a, which remained unloaded, produced the highest residual stresses.

No residual stresses were measured on grey castings, however they were used to determine the test loads for SG castings.

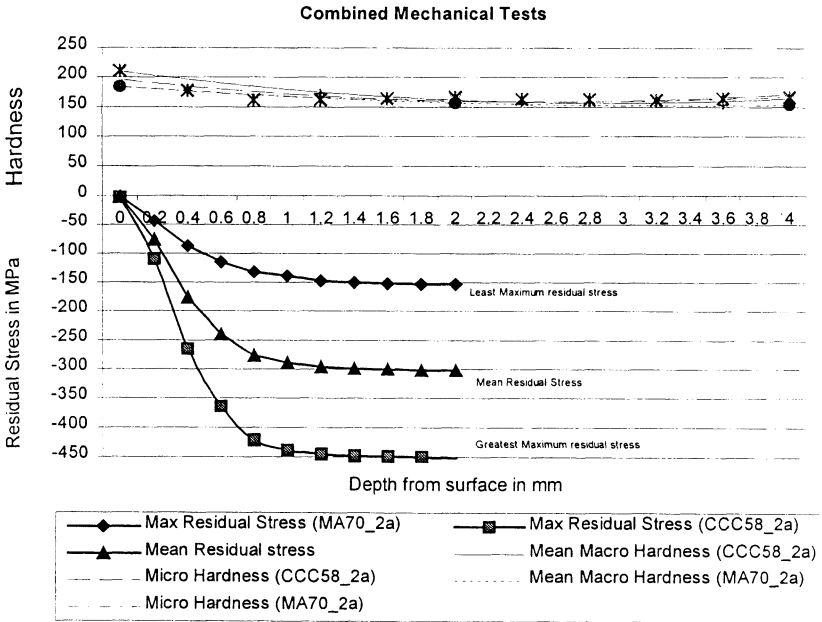

Figure 6: Combined Results showing the Micro and Macro Hardnesses and the Extreme and Mean Residual Stresses.

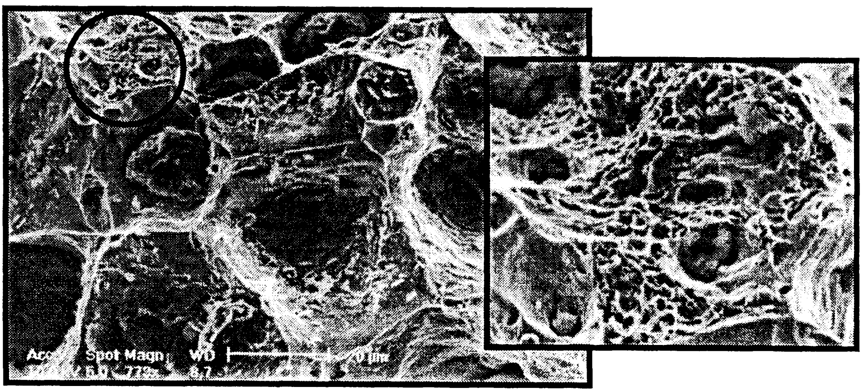

Figure 7: SEM micrograph illustrating the fracture surface at 773x magnification of Charpy Impact V-Notch test specimen with a 2319x magnification of the circled area.

Figure 7 shows the fracture modes of a ferritic ductile iron that was tested in a Charpy Impact Test at ambient temperature. The only modes of fracture visible was ductile tearing and microvoid coalescence[iv]. The dull fracture surface can be considered as a 100% shear surface according to ASTM E23[v]. All the Impact specimens exhibited the same mechanical behaviour and fracture surface.

5 Discussion

The fundamental comparison in this investigation was between unloaded and loaded components and the result of these loads on the residual stresses, hardness and impact values.

The Macro hardness results were evaluated at three areas around the drilled hole; on the surface, 2mm and 4mm below the surface, with four hardness values taken at each level, as illustrated in figure 8. The average macro hardness values at each depth was then plotted as illustrated on the hardness plot in figure 6.

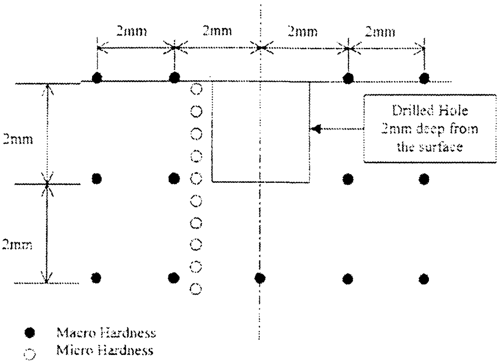

Figure 8: Area around the drilled hole where the macro and micro hardnesses were taken.

Ten micro hardness readings were also recorded at an average of 0.2mm from the edge of the hole and from a depth of 0.4mm to 4mm. Figure 6 indicates the mean micro hardness results projected to the surface.

It was observed that the average hardness for both the micro and macro hardness and for the loaded and unloaded specimens were all within 2% at a depth of 4mm while at 2mm there was an 8% difference between the two hardnesses. The graph in figure 6 indicates a steady decline in the macro hardness corresponding to the residual stresses with depth; it also depicts the micro hardness having a more rectilinear trend showing less change in hardness with depth next to the hole. This shows a constant hardness from the surface to 4mm depth, confirmed by the final macro and micro hardness values being within 3% of each other.

Transactions on Engineering Sciences vol 25, © 1999 WIT Press, www.witpress.com, ISSN 1743-3533

Examination of the ½ size Charpy Impact specimen fracture surfaces indicated that all the fractures exhibited a 100% shear surface according to ASTM E23. The trend of Lateral Expansion showed a range of 0.36mm to 0.52mm with an average of 0.46mm. The trend continued for the Impact Energy, having a minimum value of 8.5J and a maximum of 10J.

These results remained constant irrespective of the components being subjected to the test load or not.

The nature of SG Cast Iron complicates the evaluation of residual stresses, as illustrated in figure 5, as it is an anisotropic material as shown in figure 9. The mechanical and metallurgical properties of SG castings are influenced during manufacture by a number of process parameters such as, the cooling rate, ambient temperature, surface and heat treatments and rate of solidification. For this reason, the range in figure 5 was determined within which all acceptable residual stress values should fall.

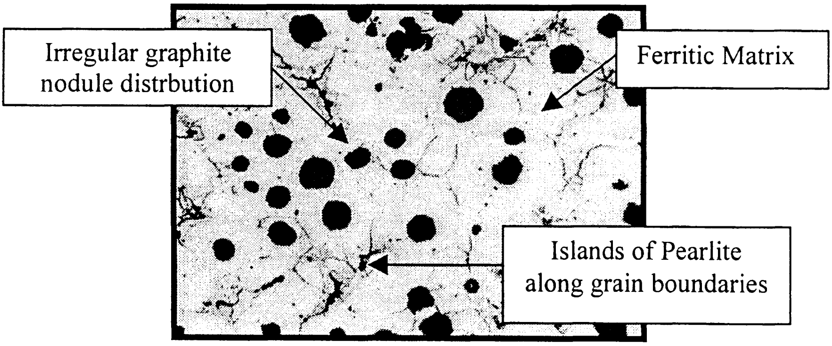

Figure 9: Micrograph of Ferritic SG Cast Iron at 220x magnification

On comparing residual stress and macro hardness it was observed that where the residual stresses were high, so too were the hardness values at the surface. This leads to the assumption that residual stresses in SG cast iron can be approximated by estimating the Ultimate Tensile Stress (UTS) from the hardness values using the ASTM A370 Table 2B[iii]. The Yield Stress can then be approximated from the UTS and the Maximum Residual Stress ≈ 0.7 x Yield Stress[vii].

Therefore a maximum residual stress may be estimated from the surface hardness. Not taking into account any surface hardening processes.

This however was not a primary focus of this investigation and warrants further investigation with respect to SG Cast Iron.

The above data was used for the development of a procedure for the testing process which in its simplest form is, that for a specific casting, if the specified test load is applied, it would result in the failure of a grey cast component but not induce detrimental residual stresses into a SG casting.

6 Conclusion

The results obtained for the loaded specimens fall within the typical range of residual stresses found in the unloaded specimens tested. Therefore, it can be concluded that loading the components to their pre-determined test loads will have no detrimental effect on the residual stresses in the SG Castings, but would result in the failure/destruction of a grey casting. This was further proved by the tests carried out on the hardness and the Impact resistance of the test components, which revealed negligible differences between loaded and unloaded components.

Out of this investigation there has arisen a number of research opportunities that could be addressed in the future, for example, the relationship between residual stresses and surface hardness in SG Cast Iron.

7 Acknowledgements

1. National Research Foundation, Industrial Partner and the Port Elizabeth Technikon for their financial assistance.
2. Mr P McGrath, PE Technikon for technical assistance.
3. Mr T Tonkin, for the manufacture of test specimens.
4. Manufacturing Research Center, Port Elizabeth Technikon.

8 References

[i]Releigh, N.C. *Measurement of Residual Stresses by the Hole-Drilling Strain Gage Method*, Tech Note TN-503-4, Measurements Group, 1993.

[ii] Hattingh, D.G, du Preez, K.H. *The analysis of process effects of 55Cr3 spring steel on residual stresses and the relation to fatigue properties*, Surface Treatment. Computational Mechanics Publications, 1997, p209-218

[iii]Sines, G. Carlson, R. *Hardness Measurement for Determination of Residual Stresses*, ASTM Bulletin, 1952, p35-37

[iv]ASM Metals Handbook 9th edition, *Fractography*, vol 12, 1987

[v]*Standard Methods for Notched Bar Impact Testing Metallic Materials*, E23, Annual Book of ASTM Standards, July 1988.

[vi]*Standard Test Method for Determining Residual Stresses by Hole Drilling Strain-Gage Method*, E837-94a, Annual Book of ASTM Standards, August 1994.

[vii]Mordfin, L. *Measurement of Residual Stresses: Problems and opportunities.* National Bureau of Standards.